Micromixers Simulation

Andrey A. GAVRILOV[1], Alexander A. DEKTEREV[1,2], Andrey V. MINAKOV[2], Valery Ya. RUDYAK[3,4,*]

Corresponding author: Tel.: +7 383 2668014; Email: valery.rudyak@mail.ru
1 Institute of Thermophysics SB RAS, Novosibirsk, Russia,
2 Polytechnic Institute of the Siberian Federal University, Krasnoyarsk, Russia,
3 Baker Hughes Inc., Russian Science Center, Novosibirsk, Russia
4 Novosibirsk State University of Architecture and Civil Engineering, Novosibirsk, Russia

Abstract A method for simulating fluid flows in microchannels is proposed. The method is tested using available experimental data obtained in micro-PIV studies of microchannel flows. Flow regimes in Y- and T-type micromixers are studied. Passive and active mixers are considered. The dependence of the mixing efficiency on the Peclet number is examined, and the possibility of using hydrophobic and ultrahydrophobic coatings is analyzed. An active mixing method using a T-mixer with a harmonically varying flow rate at one of the inlet channels is studied. The dependence of the mixing efficiency on the frequency and amplitude of flow rate variation is determined.

Keywords: Microchannels, Micromixers, Hydrodynamics, Active and Passive Mixing, Pressure Drop

1. Introduction

Fluid mixing in microchannels is an extremely important problem in various applications of microflows. In macroscopic flows, mixing usually occurs in a turbulent flow regime. Microflows, however, are usually laminar and mixing under standard conditions involves only molecular diffusion processes. Because of the extremely low values of the molecular diffusion coefficient D ($D \sim 10^{-9} \div 10^{-11}$ m^2/sec) this channel of fluid flow mixing is extremely inefficient. To increase the mixing rate, it is necessary to use special devices – micromixers. Micromixers are therefore key devices in various MEMS applications.

There are passive and active methods of increasing the mixing rate. In the first case, the geometrical shape of the channels is varied; various types of inserts are used, etc. In the second case, various external fields (acoustic, electric, magnetic) are applied, and the fluid rate is varied. The purpose of the present work is to develop a method for simulating microflows based on solutions of hydrodynamic equations and to study the mixing efficiency for both mixing methods. Several types of mixers are considered. There are some algorithm to solve this problem (see, for example, the papers Shapiro and Drikakis (2005), and Kalweit and Drikakis (2008)). In present paper the flows are simulated using the software package for solving the Navier–Stokes equations developed by Rudyak et al. (2008) and Minakov et al. (2008). This package has been tested on available data obtained using the micro-PIV technique (micro-diffuser flow, micro-separator flow, Y-shape mixers). Both stationary and quasistationary flows with tunable velocity profiles are considered. To study the effect of hydrophobic or even ultrahydrophobic coatings on mixing and pressure drop the slip boundary conditions are used.

2. Numerical Simulation Method

2.1. Analysis of the applicability range of the hydrodynamic description of microflows

It is known that, under normal conditions, flows of both liquids and not very rarefied gases can be described by methods of continuum mechanics. For microchannels, however, the situation changes drastically. The term microchannel usually refers to a channel in which one of the characteristic sizes h (for example, the height of a flat channel or the diameter of a cylindrical channel) is in the

range from 1 to approximately 300 μm. Under these conditions, liquid and gas flows should be described differently, as a rule. Indeed, if the gas is not too dense (up to pressures of approximately 10–20 atm.), the corresponding Knudsen number of such microflows varies in the range $10^{-2} \le \mathrm{Kn} \le 10^{2}$. At these Knudsen numbers, flows can no longer be described by hydrodynamic equations. More precisely, at the lower limit, it is still possible to use the Navier–Stokes equations but with the slip boundary conditions. In simulations down to Knudsen numbers $Kn \sim 10^{-1}$, it is necessary to use the Burnett equations, and then, the Boltzmann kinetic equation.

The continuum concept for liquids is valid if it is possible to distinguish a hydrodynamic physically infinitesimal scale r_h such that the fluctuations in the corresponding volume can be ignored. For a liquid, $r_h \sim \sqrt{dh}$, (Rudyak, 1995), where d is the characteristic size of the liquid molecule. If the microchannel height is $h \sim 1$ μm, we have $r_h \sim 2 \cdot 10^{-6}$ cm, which is comparable to the channel height. Therefore, in the presence of gradients of macroscopic variables in such flow, the hydrodynamic description will fail. Difficulties arise even with the introduction of macroscopic variables, which, by the definition, are the averages over a physically infinitesimal volume of the corresponding dynamic variables of the molecular system.

Special problems arise near the channel walls. In gases, viscosity is related to the momentum transfer by molecules and, therefore, it forms on scales larger than the mean free path of molecules. In liquids, short-range order exists on scales of the order of 1 nm and viscosity occurs on mesoscales of $r_l > d$. Thus, the viscous fluid model is valid only for scales beginning with a few tens of nanometers. Therefore, in microchannels, the fluid viscosity near the walls can be different from that in the bulk. In addition, transport processes in small microchannels cease to be isotropic. For example, molecular diffusion along the channel differs from that across the channel.

The situation is further complicated for two-phase fluids in microchannels. Microflows of nanofluids at low volume concentrations of nanoparticles ($\phi \le 10^{-4}$) can be described using one-fluid hydrodynamics. In this case, however, it is necessary to introduce effective transport coefficients. In addition, the traditional no-slip boundary conditions are no longer applicable in this case, and surface structure, in particular, its roughness gain in importance. It should also be noted that, with increasing volume concentration of nanoparticles, the medium can change rheological properties and become non-Newtonian. If the characteristic size of the dispersed particles reaches $10^{-4} \div 10^{-5}$ cm (Brownian particles), the hydrodynamic description for small microchannels becomes absolutely inappropriate. In this case, it is necessary to use a mixed description with a coupled system of kinetic-hydrodynamic equations (Rudyak, 1999) in which the carrier medium is described by hydrodynamic equations with interfacial forces and the dispersed phase by the kinetic equation.

2.2. Algorithm for the solution of the Navier–Stokes equations and its testing

In the present work, fluid microflows are described within the framework of the continuum model using the Navier–Stokes equations with no-slip or slip boundary conditions. Multicomponent flow is simulated using the one-velocity hydrodynamics. The incompressible flows with variable density are considered. Their dynamics is governed by the following equations

$$\frac{\partial \rho}{\partial t} + \nabla \cdot (\rho \mathbf{v}) = 0, \qquad (2.1)$$

$$\frac{\partial \rho \mathbf{v}}{\partial t} + \nabla \cdot (\rho \mathbf{v}\mathbf{v}) = -\nabla p + \nabla \mathbf{T}, \qquad (2.2)$$

where ρ is the fluid density, p is the pressure, $\mathbf{v}$ is the fluid velocity, and $\mathbf{T}$ is the viscous stress tensor. The density of the mixture is expressed in terms of the mass fractions f_i of the flow components and the

partial densities ρ_i

$$\rho = \left[\sum_i (f_i / \rho_i) \right]^{-1}.$$

The transport equation for the components of the mixture in mass fractions is written as

$$\frac{\partial \rho f_i}{\partial t} + \nabla \cdot (\rho f_i \mathbf{v}) = \nabla \cdot (\rho D_i \nabla f_i), \quad (2.3)$$

where D_i is the diffusion coefficient of the i-th component. The difference analog of the convection-diffusion equations (2.1)–(2.3) is found using a finite-volume method (Ferziger and Peric, 2002) for structured multiblock grids. In this case, the resulting scheme is automatically conservative. The method consists of partitioning the calculated domain into control volumes with the subsequent integration of the initial conservation equations over each control volume to obtain finite-difference relations.

The convective terms of the transport equations (2.2) and (2.3) are approximated by the second-order counterflow QUICK (Leonard, 1979) and TVD schemes (Lien and Leschziner, 1994.), respectively. A second-order implicit scheme is use to approximate the unsteady terms of the hydrodynamic equations.

Diffusion fluxes and source terms are approximated by finite-volume analogs of the central-difference relations of second-order accuracy. The coupling between the velocity and pressure fields, which provides satisfaction of the continuity equation (2.1), is achieved by the SIMPLEC algorithm on aligned grids (Patankar, 1980). Oscillations of the pressure fields are prevented using the Rhie-Chow method involving the introduction of a pressure smoothing term into the equations for pressure correction (Patankar, 1980). The difference equations obtained by discretization of the initial system of differential equations are solved by an iterative method using an algebraic multigrid solver.

The algorithm described here has been employed to solve a wide range of problems of external and internal flow (Minakov et al., 2008; Rudyak et al., 2008). Convergence of the iteration process to a stationary solution is achieved after about 1500 iterations for low Peclet numbers (Pe < 1000) and about after 4000 for high Peclet numbers (Pe > 20000). At the same time, its applicability to the description of microflows required special testing. Three examples of such testing are given in the present section.

Let us consider Newtonian fluid flow in a microdiffuser (Wing and Rajan, 2004). The channel height is h = 100 μm, the width of the narrow part of the channel is w = 150 μm, and that of the wide part is W = 750 μm. The fluid moves from the narrow part of the channel to the wide part. No-slip conditions are imposed on the solid walls. At the inlet, the fluid flow rate corresponding to Reynolds number $\mathrm{Re} = 1$ is specified. Figure 1 shows a comparison of experimental data (Wing and Rajan, 2004) with the dimensionless velocity profile U/U_m (U_m is the maximum flow velocity in the given section) calculated using the proposed method for solving the Navier–Stokes equations. The experimental data (filled circles) were obtained for the wide part of the diffuser using the micro-PIV technique. The calculated data (solid curve) are in good agreement with the experimental data over the entire flow region.

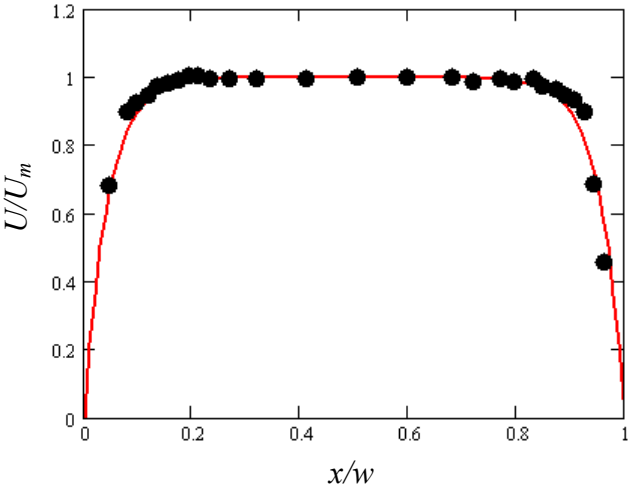

Fig. 1. Comparison of calculated and experimental values of the longitudinal flow velocity in a diffuser.

The next test example is also taken from paper (Wing and Rajan, 2004). The microchannel

presented in Fig. 2 is considered. The channel has identical height and width equal to 100 μm. No-slip conditions are imposed on the solid walls. The Reynolds number constructed from the flow rate at the channel inlet is $\mathrm{Re}_Q = 1$. Figure 3 shows a comparison of the calculated (solid curves) and dimensionless measured (filled circles) velocity profiles. The dimensionless velocity profile is obtained by normalization to the velocity determined by the flow rate Q at the inlet: $U_Q = Q/\rho S$, where S is the cross-sectional area of the microchannel. The measurements and calculations were performed in sections A (curve 1) and B (curve 2). In this case, there is also good agreement between the calculated and measured data.

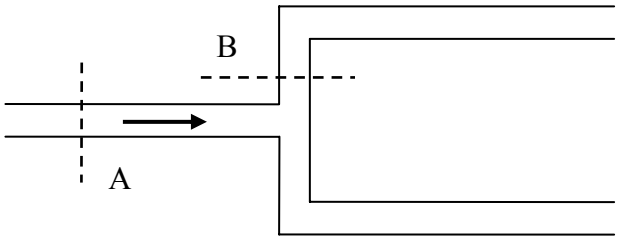

Fig. 2. Diagram of microflow in a tee junction.

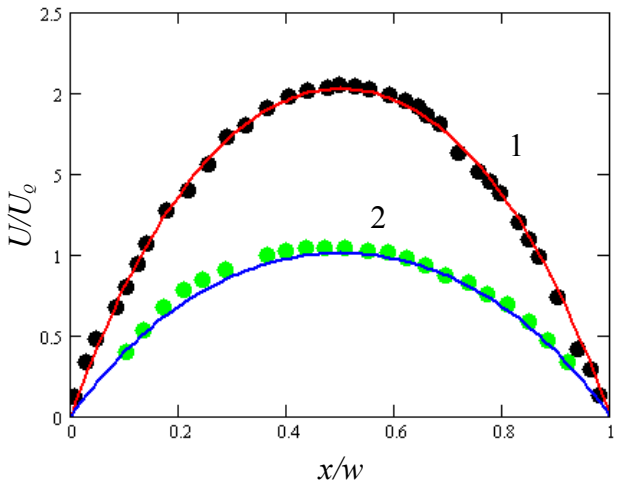

Fig. 3. Comparison of calculated and normalized experimental values of the longitudinal flow velocity in a microtee junction.

Finally, we give one more test example for flow in the Y-type micromixer shown schematically in Fig. 4. Kim et al. (2003) studied mixing of water (inlet B) and a glycerol solution (inlet A). Channels A and B were each 150 μm wide, and the mixer was 300 μm wide. The heights of the channels were identical and equal to 50 μm. In the experiment, the angles α and β were equal. In experiment (Kim, Liu and Sung, 2003), water was mixed with 20 %, 50 %, and 60 % glycerol solutions, whose density and viscosity coefficient increase successively. In all cases, the calculation is in good agreement with the experimental data. Figure 5 gives a comparison of the longitudinal flow velocity profile in section C. Here, as before, the solid curve corresponds to calculated data and filled circles to experimental data.

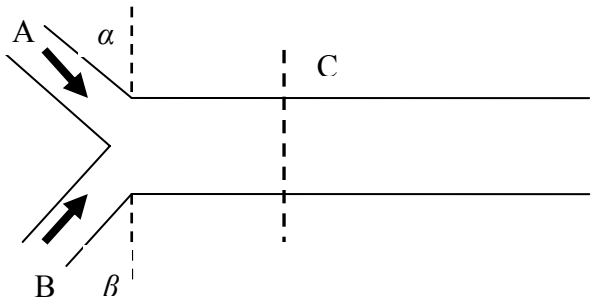

Fig. 4. Diagram of an Y-type micromixer.

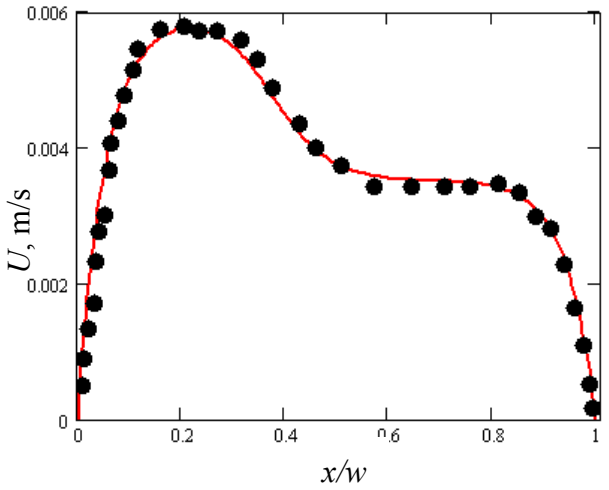

Fig. 5. Comparison of calculated and experimental values of longitudinal flow velocity in section C (see Fig. 4).

3. Mixing in an Y-type Mixer

An Y-type micromixer is one of the simplest models. Mixing in this micromixer has been studied extensively during the recent decade. However, systematic data on the effect

of mixing on flow parameters are not available. For this reason, we start the investigation of micromixers from this model.

So, we consider the mixing of two identical fluids, for example, a blue and a red fluids in the micromixer presented in Fig. 4. Let, for definiteness, the blue fluid enters channel B, and the red fluid enters channel A. If the flow rates in both inlet channels are identical, the flow Reynolds numbers in channels A and B are identical and equal to $\mathrm{Re}_w = \rho U_Q w/\mu$, where μ is the viscosity coefficient of fluid. The mixing time is determined only by the fluid diffusion coefficient D and is of order $\tau_m \sim w^2/D$. If the channel has length L, the time required for a fluid particle to pass through the channel is of order $\tau_L \sim L/U_Q \sim$ $\sim (\rho L w h)/Q$. The mixing efficiency in the channel is determined by the ratio of these two times

$$\frac{\tau_m}{\tau_L} \sim \frac{w^2 U_Q}{DL} \sim \frac{w}{L}\mathrm{Re}_w \frac{\nu}{D}, \qquad (3.1)$$

where $\nu = \mu/\rho$ is the kinematic viscosity coefficient. Therefore, for the given channel and given fluids, the mixing time is proportional to the Reynolds number. If one uses water as the fluids being mixed, then, according to (3.1), the mixing in a channel of length $L = 1$ cm is efficient if $\tau_m < 10\,\mathrm{Re}_w \tau_L$, which is valid only for very small Reynolds numbers. From this, in particular, it follows that, starting from some values of the Reynolds number, the mixing efficiency changes little.

From Eq. (3.1), it is easy to obtain the estimate

$$\frac{\tau_m}{\tau_L} \sim \frac{w}{L} Pe, \qquad (3.2)$$

where Pe is the Peclet number $Pe = wU_Q/D$ (or the diffusion Peclet number). For a given Peclet number, the mixing length $L_m \sim U_Q \tau_m \sim Pew$ is the smaller the smaller the channel width, and this length increases with increasing Peclet number.

It should be noted, however, that the dependence of the mixing efficiency on the Peclet number is nonlinear. It is given in Fig. 6 for Y-mixer considered (Fig. 4). Here the mixing efficiency M is determined by the formula

$$\mathrm{M} = \left[1 - \frac{2}{W}\int_0^W (C - 0.5)dy\right] \cdot 100\%,$$

where $W = 300$ μm is the width of the channel in which mixing occurs (Fig. 4) and C is the color concentration in the section at 4000 μm from the site of flow merging. This dependence is well described by the formula

$$\mathrm{M} = \frac{113.2}{1 + 0.037\,Pe^{0.7}}.$$

In Fig. 6, it is shown by the solid curve and the points correspond to calculations.

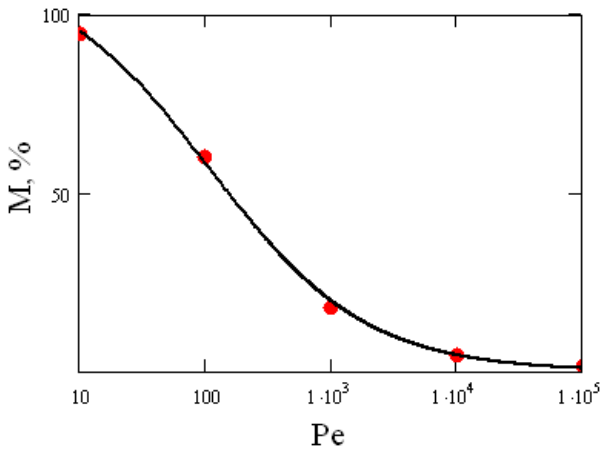

Fig. 6. Mixing efficiency in a Y-type mixer versus Peclet number.

Next, we studied the effect of the angles α and β. Both angles were varied from 0° to 90° (see Fig. 4). The degree of opening of channels A and B was found to have little effect on the mixing efficiency.

Since diffusion is the most important factor of the mixing process in microchannels, the channel length should be sufficiently great to provide flow mixing. Naturally, this leads to a significant pressure drop due to friction on the channel walls. On the other hand, it is obvious that such losses are much lower in the case of

flow slip rather than no-slip conditions on the channel walls. At the macroscopic level of description, the boundary conditions are always specified as no-slip conditions. Slip boundary conditions are employed only to describe flows of fairly rarefied gas. This is due to the fact that, in a gas, the characteristic wall slip length b is of the order of the Knudsen number $b \sim Kn$ (here slip length b is determined by the following relation $v = b(\partial v / \partial x)$, where v is the flow velocity along the x axis).

In macroscopic fluid flows under usual conditions, the slip length varies from a few nanometers to several tens of nanometers. This slip can be ignored. In microflows, however, such slip can be significant. In addition, in microflows, the slip length can reach a few hundred nanometers. This is related to a change in the short-range order of fluid near surfaces, the possibility of gas release on the channel walls, etc.

Table 1. Parameters of the mixing liquids

	ρ, k/m^3	μ, Pa sec	D×10^{-9} m^2/sec
Acetone	800	0,00029	4,56
Glycerol	1260	1,48	0,0083
Ethanol	790	0,0012	1,24
Isopropyl alcohol	786	0,0029	0,38

Walls slip leads to a significant decrease in the friction drag on the channel walls and, hence, to a reduction in the pressure drop. To increase the slip length, it is common to use various hydrophobic or even ultrahydrophobic coatings (see, for example, Ou, Perot and Rothstein, 2004; Lauga, Brenner and Stone, 2005). In this case, the slip length can reach tens of micrometers. Systematic calculations performed for a Y-type micromixer (Fig. 4 see) have shown that as the slip length increases to 5 μm, the pressure loss decreases by almost half. It should be emphasized that, in the presence of wall slip, the mixing efficiency changes only slightly.

Till now we discussed the mixing of the same fluids. In practice the mixing the different liquids is interesting. Certainly our algorithm permits to study these situations too. As an example we present the mixing the water with different liquids (see table 1) in Y-type mixers. The water is supplied through the entry A (Fig. 4). Because the physical characteristics of these liquids are very different the mixing efficiency is essentially differed too. In particular, the parameter M for acetone, glycerol, ethanol and isopropyl alcohol is equal to 36%, 3%, 18% and 9%, respectively. In these cases the pressure drop between exits A and B is different and it is changes from 239.5 kPa for the glycerol till 165 Pa for acetone.

4. Mixing in a T-type Mixer with Inserts

Relations (3.1), (3.2) give an estimate of the mixing time and length and, hence, the efficiency of micromixers. From general considerations, it is clear that the mixing time can be reduced considerably by multiply splitting the mixing flow. This principle underlies the design of lamination mixers (see, for example, Karnik, 2008). A similar idea is to place a number of obstacles in mixing flow to change the flow structure and thus to accelerate mixing. It is clear that, in laminar flow, symmetric arrangement of obstacles is less effective.

Table 2. Mixing efficiency and pressure loss in a mixer with rectangular inserts

N	M %	Δp, Pa
0	6.6	260
3	20.7	730
5	27.1	1100
7_1	33.1	1400
7_2	61.9	5387

In addition, the characteristic size of the obstacles should be comparable to the sizes of the channel. Moreover, the mixer is easy to optimize for this parameter. Series of such calculations for mixers of various types were performed in the present work.

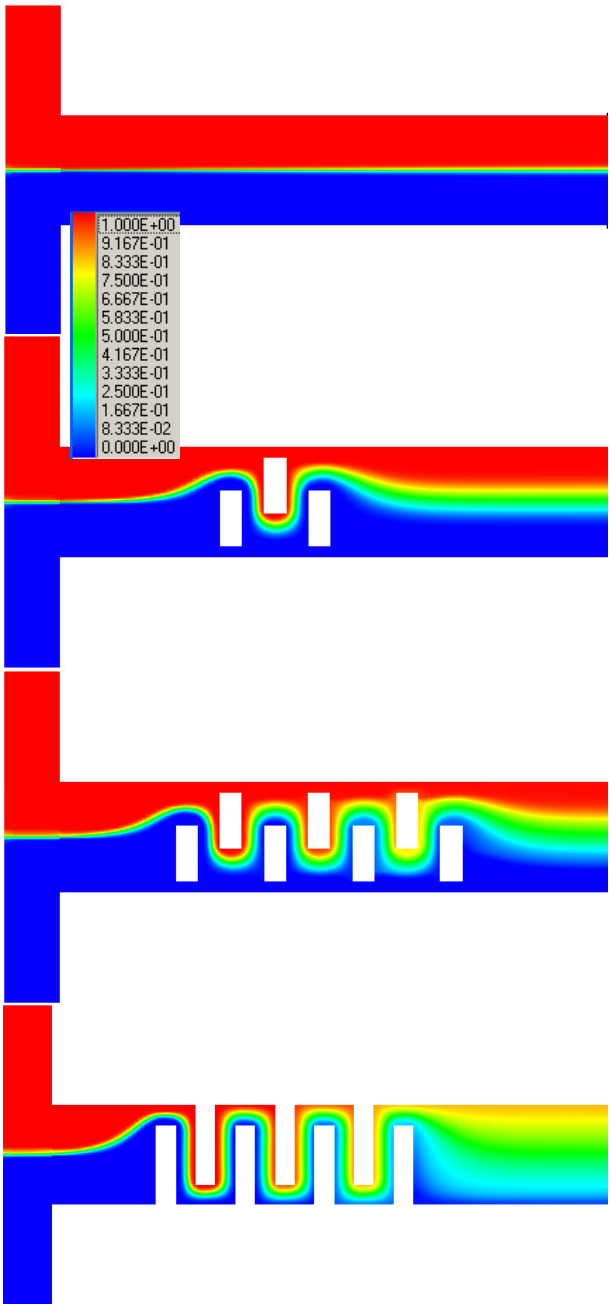

Fig. 7. Comparison of mixing of two fluids (red and blue) in a mixer of T-type with asymmetrically arranged inserts.

As an example, Figure 7 shows mixing of two fluids in a mixer with asymmetrically arranged three and seven rectangular inserts and without inserts. The mixing channel is 100 μm wide, the inlet channels are 50 μm wide, and the channel height is 50 μm. The Reynolds number Re = 2, and the Peclet number $Pe = 5 \cdot 10^3$. All inserts are identical and have a cross-sectional area of 50 μm×20 μm. Data on the mixing efficiency are presented in Table 2.

The mixing efficiency increases with increasing number of inserts, but the pressure loss also increases. It can be reduced by using hydrophobic coatings. Thus, for a slip length $b = 1$ μm, the pressure loss can be reduced by 10%. The mixing efficiency can be increased if the inserts connect with the wall. Such situation presents on the last picture in Figure 7. Here the length of the insert is equal to 70 μm (last row in table 2).

5. Active mixing method

One of the simplest methods of active mixing in Y- and T-type mixers is the one with periodic variation in the flow rate at one (or at the both) of inlets. In the present work, the velocity U_Q was varied. It was given by the relation

$$U_Q = U_0 + V \sin 2\pi f t . \qquad (5.1)$$

The parameters included in expression (5.1) are generally determined by the characteristic sizes of the mixing channel and flow characteristics (Reynolds and Peclet numbers). It is clear that, if the characteristic mixing time is much smaller than the period of flow rate variation $\tau_m << 1/2\pi f = T_f$ or $\tau_m \sim T_f$, this will hardly change the mixing efficiency in comparison with stationary mixing. Therefore, it is the most reasonable if $\tau_m >> T_f$. On the other hand the period of flow rate has to be less than the characteristic flow time $T_f < \tau_L$. The optimum amplitude of variation is easy to estimate by considering the volume of mixed fluids during the period of flow rate variation.

These qualitative considerations are also supported by direct calculations. As an example we will present the calculations data for the mixer with the following parameters: $w = 200$ μm, $L = 2000$ μm, $U_0 = 10^{-3}$ m/c. We analyzed the mixing the fluid with the viscosity coefficient $\mu = 6.67 \cdot 10^{-4}$ Pa·sec and the diffusion coefficient $D = 7 \cdot 10^{-11}$ m²/sec which corresponds to Re = 0.3 and $Pe = 3000$. For the given parameters,

$\tau_m \sim 560$ sec and $\tau_L \sim 2$ sec. Therefore the optimal frequency should be satisfied to the condition $T_f < 2$ sec. The corresponding frequency is determined by the following condition $f_{op} > 0.08\,\text{Hz}$. This estimation gives the following flow rate frequency: $f_{op} \sim 1\,\text{Hz}$. As an example of corresponding calculations, Fig. 8 shows the dependence of the mixing efficiency on the frequency f and amplitude V. The mixing of two fluids in a T-type micromixer is considered. Here the red, black, brown and blue points and lines correspond to values of V equal to 1, 2, 5, and 10 mm/sec, respectively. Really, the optimal mixing is achieved at frequency of the order of 1 Hz.

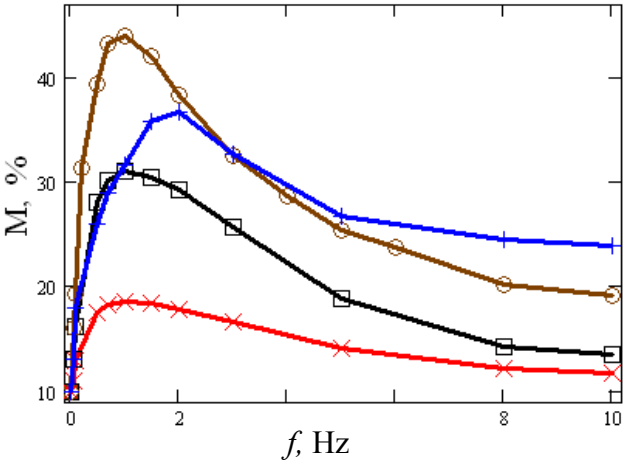

Fig. 8. Mixing efficiency versus frequency f and amplitude V.

Acknowledgments

This work was supported in part by the Russian Foundation for Basic Researches (grant No. 07-08-00164) and by the grant of the President of the Russian Federation for Support of Leading Scientific Schools (project no. NSh-454.2008.1).

References

Ferziger J.H. and Peric M. 2002. Computational methods for fluid dynamics. Springer Verlag, Berlin.

Kalweit M. and Drikakis D. 2008. Multiscale methods for micro/Nano flows and materials. J. Comp. & Theoretical Nanoscience. 5, 1923–1938.

Karnik R. 2008. Microfluidic mixing encyclopedia of microfluidics and nanofluidics. Ed. Li D. Springer. P. 1177–1186.

Kim WJ., Liu Y.Z. and Sung H.J. 2003. MicroPIV in two-fluid flow. Proc 5th Int. Symp. on Particle Image Velocimetry. Busan.

Lauga E., Brenner M.P. and Stone H.A. 2005. Microfluidics: the no-slip boundary condition. Handbook of experimental fluid dynamics. Eds. Foss J., Tropea C., and Yarin A. Ch. 15.

Leonard B.P. 1979. A stable and accurate convective modeling procedure based on quadratic upstream interpolation. Comp. Math. Appl. Mech. Eng. **19**, 59–98.

Lien F S. and Leschziner M. A. 1994. Upstream monotonic interpolation for scalar transport with application to complex turbulent flows. Int. J. Num. Math. Fluids. **19,** 527–534.

Minakov A. V., Gavrilov A. A., Dekterev A. A. 2008. Numerical algorithm for solving spatial problems of hydrodynamics with moving solids and a free surface. Siberian J. Industrial Math. **11**, # 4(36), 94–104.

Ou J., Perot B. and Rothstein P. 2004. Laminar drag reduction in microchannels using ultrahydrophobic surfaces. Phys. Fluids. **16**, 4635–4643.

Patankar S.V. 1980. Numerical heat transfer and fluid flow. Washington, DC, Hemisphere, 1980.

Rudyak V.Ya. 1995. Nonlocality solution of the Boltzmann equation. Sov. Phys.-Tech. Phys. **40**, # 11, 29–40.

Rudyak V.Ya. 1999. Mixed kinetic-hydrodynamic level of description for dispersed liquids. Tech. Phys. Lett. **25**, 900–901.

Rudyak V.Ya., Minakov A.V., Gavrilov A.A., Dekterev A.A. 2008. Application of new numerical algorithm of solving the Navier–Stokes equations for modeling the work of a viscometer of the physical pendulum type. Thermophysics & Aeromechanics. **15**, 333–345.

Shapiro E. and Drikakis D. 2005. Artificial compressibility, characteristics-based schemes for variable density, incompressible, multi-species flows. Part I, Part II. J. Comp. Phys. **210**, 584–607; 608–631.

Wing T.L., Rajan K.M. 2004. Flow measurements in microchanells using MicroPiIV system Proc. 15th Australian Fluid Mechanics Conference. The University of Sydney, Sydney.